ACS SENSORS

pubs.acs.org/acssensors
Letter

Systematic Mutation and Unnatural Base Pair Incorporation Improves Riboswitch-Based Biosensor Response Time

Sudeshna Manna, Michiko Kimoto, Johnny Truong, Praneeth Bommisetti, Ava Peitz, Ichiro Hirao,* and Ming C. Hammond*

Cite This: *ACS Sens.* 2023, 8, 4468−4472

ABSTRACT: Engineered RNAs have applications in diverse fields from biomedical to environmental. In many cases, the folding of the RNA is critical to its function. Here we describe a strategy to improve the response time of a riboswitch-based fluorescent biosensor. Systematic mutagenesis was performed to either make transpose or transition base pair mutants or introduce orthogonal base pairs. Both natural and unnatural base pair mutants were found to improve the biosensor response time without compromising fold turn-on or ligand affinity. These strategies can be transferred to improve the performance of other RNA-based tools.

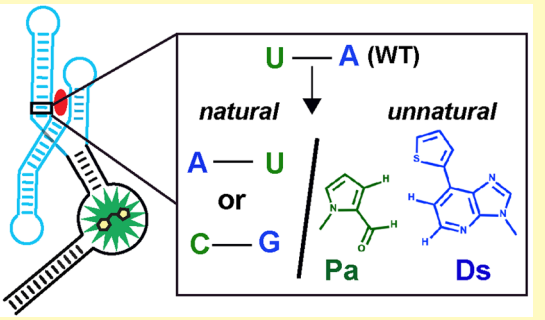

KEYWORDS: *RNA-based fluorescent biosensors, guanidine, riboswitch folding, base pair mutagenesis, orthogonal base pairs, rapid sensing*

Natural and synthetic RNA tools have been developed for diverse applications, including diagnostics, therapeutics, imaging, and genome editing.[1,2] Each of these functions requires the RNA to be in a specific conformation, which could be single-stranded, double-stranded, structured, or a combination. In some cases, the RNA must undergo conformational changes to form an active complex or to interact with a molecular target. Thus, folding is critical to the activity of the RNA-based tools.

Riboswitches are natural structure-switching RNAs that recognize small molecule ligands with high specificity and affinity and can be fused to fluorogenic aptamers to make RNA-based fluorescent (RBF) biosensors.[3,4] While researchers mainly have focused on selectivity and sensitivity in biosensor design, recently, we have been interested in understanding and overcoming limitations in RNA-based biosensor response time.[5] Access to faster biosensors would expand their capabilities for both real-time diagnostic and molecular imaging applications.

We hypothesized that because riboswitches are evolved for gene regulation, the natural sequences are selected for structural switching in the context and timing of that cellular process, which does not necessarily optimize for rapid ligand sensing. Thus, we explored ways to identify biosensor sequences with faster response times. Here we show that riboswitch conformational change is the rate-determining step for an RBF biosensor. Two structure-based approaches were developed, systematic mutagenesis and orthogonal base pair incorporation that lead to biosensors with substantially improved response times. To the best of our knowledge, this study is the first to synthesize and analyze an RNA-based fluorescent biosensor incorporating unnatural orthogonal base pairs.

We recently reported an RBF biosensor for the metabolite and environmental pollutant, guanidine, that gets activated within a few minutes of analyte addition both *in vitro* and *in vivo* (Figure 1A, Supporting Information (SI), Figure S1).[5] In contrast, the fluorogenic aptamer by itself, Spinach2, displays much faster fluorescence turn-on (SI, Figure S2A) and was previously shown to be preorganized for dye binding.[6] The slower turn-on response of the biosensor is due to its fluorogenic mechanism, which requires that the riboswitch−ligand interaction controls folding of the fluorogenic aptamer to affect dye binding. Accordingly, preincubation of the biosensor with guanidine to form the riboswitch−ligand complex partially restores fast turn-on (SI, Figure S2B). Thus, the rate-determining step for this biosensor involves riboswitch folding upon ligand association.

A hidden aspect of biomolecular sensors, both protein and RNA-based, is that designs have to contend with misfolding, which is akin to side reactions that degrade both fold turn-on and activation rate. A general misfolding mechanism for RNA is for a region to form alternative base pairs that are not found

Received: June 23, 2023
Accepted: October 3, 2023
Published: October 25, 2023

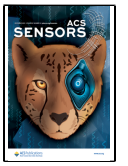

https://doi.org/10.1021/acssensors.3c01266
ACS Sens. 2023, 8, 4468−4472

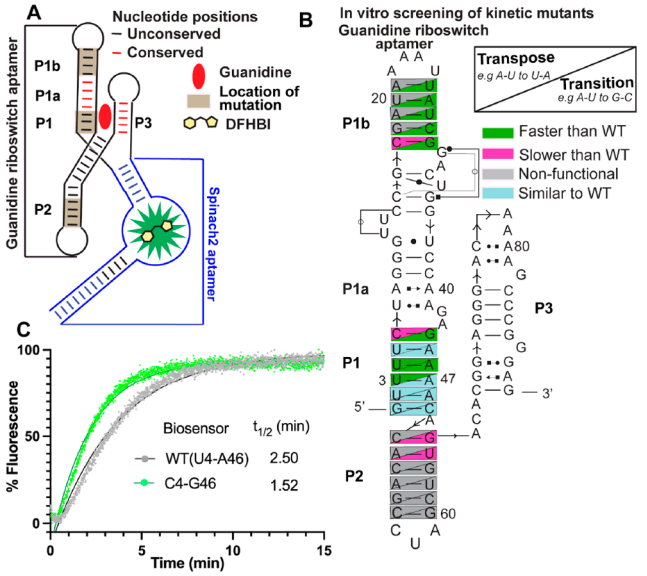

Figure 1. (A) Schematic representation of Dru J 2,2-D-guanidine biosensor. (B) *In vitro* kinetic screening results of 34 single mutants. Results for each base pair are shown for the transpose mutation (top region) and transition mutation (bottom region). (C) *In vitro* turn-on kinetic plots of the WT and C4-G46 biosensors. Scattered dots represent the data points, and solid lines represent best-fit curves.

in the final, ligand-bound structure (SI, Figure S3). Because ligand-induced folding appears to be the slowest step in biosensor activation, we hypothesized that systematically mutating single base pairs in the riboswitch can block misfolding pathways while maintaining biosensor function. Three base-pairing regions in the riboswitch (P1, P1b, and P2) were chosen that are not sequence conserved based on phylogenetic analysis and not involved in ligand recognition based on the X-ray crystal structure. Only two types of mutations were performed, transition (e.g., G-C ↔ A-U) and transpose (e.g., G-C ↔ C-G, A-U ↔ U-A), which either maintain purine−pyrimidine character or base pair stability in order to maintain biosensor function.

An initial kinetic screen of 34 base pair mutants prepared in a high-throughput manner showed that 59% of the mutant biosensors retain function (Figure 1B, SI, Figure S4 and Table S1). Interestingly, these conservative mutations at the P2 stem uniformly made the biosensor nonfunctional or slower than WT, whereas the effect of mutations at the P1b stem was strongly dependent on type, such that transposed mutants were detrimental, but transition mutants were faster than WT. Finally, mutations at the P1 stem almost uniformly made the biosensor similar or faster than WT, regardless of type.

We chose to further characterize five P1 and five P1b stem mutants shown to be faster than WT in the initial screen (SI, Figures S5 and S6 and Tables S1, and S2). Some deviation from the initial results for these RNA constructs was observed, likely due to variable RNA purities and concentrations for the high-throughput screen versus gel-purified RNA for rigorous analysis. However, two base-pairs central to the P1 stem, U3-A47 and U4-A46, showed remarkable kinetic improvements with both mutation types compared to WT ($\Delta t_{1/2}$ = 0.5−1.0 min, and k_{rel} = 1.3−1.6). In addition, two base-pairs at the top of the P1b stem-loop, U20-A27 and A21-U26, were moderately faster than WT ($\Delta t_{1/2}$ = 0.3−0.4 min, and k_{rel} = 1.1−1.2) when transition mutants were made. The fastest biosensor mutant, C4-G46, achieved 1 min faster $t_{1/2}$ and 1.6 times higher apparent rate constant than the WT (Table 1).

Table 1. Fold Turn-On and Kinetic Parameters of P1 Stem Mutants[a]

WT bp	mutant	ft	$t_{1/2}$ (min)	k_{obs} (min^{-1})	k_{rel}
WT	none	2.1	2.50 ± 0.23	0.28 ± 0.02	1.0
U3-A47	A3-U47	2.6	1.85 ± 0.19	0.38 ± 0.04	1.4
	C3-G47	2.3	1.99 ± 0.15	0.35 ± 0.03	1.3
U4-A46	A4-U46	1.9	1.59 ± 0.13	0.44 ± 0.03	1.6
	C4-G46	2.1	1.52 ± 0.16	0.46 ± 0.05	1.6
C6-G44	U6-A44	2.1	2.74 ± 0.11	0.25 ± 0.05	0.9

[a]bp = base pair, ft = fold turn-on, k_{rel} = k_{obs} (mutants)/k_{obs} (WT). All measurements performed in triplicate with 100 nM RNA, 3 mM guanidine. Standard deviation for fold turn-on was ≤0.4.

Some mutants displayed both faster turn-on and larger fluorescence activation than WT. However, ligand binding affinities for these biosensors were similar to WT (SI, Figure S7), which indicates that the mutations are not affecting the binding equilibrium, consistent with our choice of mutating regions not involved in ligand recognition. Instead, these mutants likely block misfolded intermediates that are "off-path" to the ligand-bound structure (SI, Figure S3). In contrast, other mutants in our analysis appear to block "on-path" misfolded intermediates and thus give faster turn-on only (without affecting the magnitude of fluorescence activation).

To evaluate the effect of combining the base pair mutants, we made two types of double mutants. Four double mutants combined the two P1 stem base pairs (U3-A47 and U4-A46), whereas four other double mutants combined a P1 stem base pair and a P1b stem base pair (SI, Figures S8 and S9, Tables S3 and S4). The combination of the fastest P1 and P1b stem mutants resulted in the best performing double mutant (C4-G46/C20-G27, $\Delta t_{1/2}$ = 0.7 min and k_{rel} = 1.3). However, to our surprise, none of the double mutants tested were faster than the fastest single mutant. These mutations not being additive could be due to (i) single mutants blocking the same misfolded intermediate, which seems likely for the two P1 stem base pairs, and (ii) double mutants blocking some but also generating new misfolding pathways, resulting in a net neutral or slightly positive effect on kinetics.

So far, our systematic mutagenesis strategy involved swapping one natural base pair for another, which in general risks generating new misfolding pathways. We next considered whether the incorporation of orthogonal unnatural base pairs (UBPs) could offer a novel workaround. Hydrogen bonding[7] and non-hydrogen bonding[8−10] UBPs have been developed to introduce new functionalities in nucleic acids and have been applied in a variety of applications, including generating high-affinity DNA aptamers,[11,12] PCR-based diagnostics,[13] RNA labeling,[14,15] and generating semisynthetic organisms.[16] Recently, it was shown that incorporation of two hydrogen-bonding UBPs, P−Z and B−S, at the stem region of the Spinach aptamer maintains its fluorogenic properties.[17] However, to our knowledge, UBPs have not been incorporated into RBF biosensors and have not been shown to improve their function.

https://doi.org/10.1021/acssensors.3c01266
ACS Sens. 2023, 8, 4468−4472

Non-hydrogen bonding UBPs would avoid both duplex and noncanonical base pair interactions with the standard nucleobases. Ds-Pa or Ds-Pa′ UBPs previously showed high fidelity in transcription reactions and have been applied for RNA labeling and post-transcriptional RNA modifications.[14,18] Because the systematic mutagenesis already identified hotspots for kinetic improvement, we incorporated five different UBPs in place of U3-A47 or U4-A46 by *in vitro* transcription using T7 RNA polymerase and duplex DNA containing Ds or Pa in the template strand, which was constructed by solid-phase synthesis and DNA ligation reactions (Figure 2A).

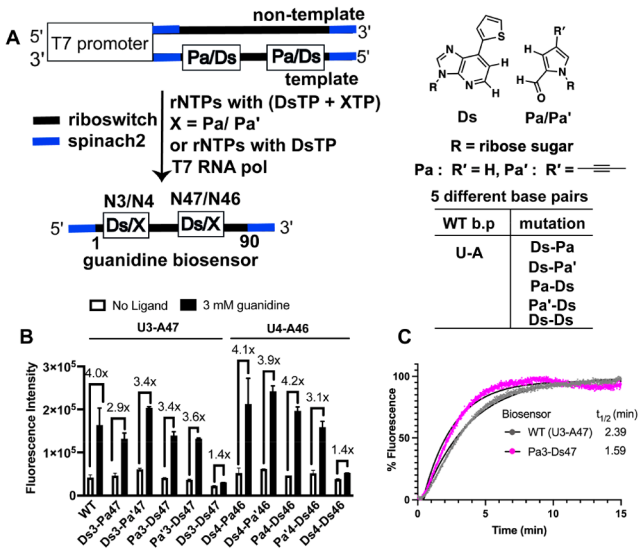

Figure 2. (A) Site-specific incorporation of Ds and Pa/Pa′ by *in vitro* transcription using synthetic DNA templates. (B) Fold turn-on of the WT and UBP containing biosensors. (C) *In vitro* turn-on kinetic plots of the WT biosensor and Pa3-Ds47 mutant. Scattered dots represent the data points, and solid lines represent best-fit curve.

UBP incorporation into the RNA-based biosensors was evaluated by LC-MS of nucleosides, polyacrylamide gel analysis of cDNA, and high-resolution mass spectrometry (HRMS) of the RNA fragments. Following breakdown of the RNA to individual nucleosides, Pa/Pa′ and Ds nucleosides were detected by LC-MS at 291 and 309 nm, respectively (SI, Figure S10). In addition, the % of Ds and Pa/Pa' nucleosides determined at 260 nm were consistent with single site incorporation (SI, Table S5).

Next, the UBP position was assessed by reverse transcription reactions on biosensor RNAs using fluorescently labeled primers and analysis of the cDNA products. Without the unnatural dNTPs, stalling was observed at each of the expected positions, but low fidelity of the reverse transcriptase for UBPs complicated the analysis (SI, Figure S11).[19] With unnatural dNTPs, full-length cDNAs are produced and partial alkaline digestion selectively cleaved the cDNA at ^{Di}Px,[20] which corresponds to Ds positions in the RNA template. The product cleavage patterns strongly support site-specific incorporation (SI, Figure S12). Finally, we directly analyzed the biosensor RNA by partially digesting with RNase T1 and analyzing the fragments by HRMS. The expected RNA fragments for Pa/Pa′ at position 3 and Ds at position 47 were detected at −2 to −4 charge states, which confirms site-specific UBP incorporation (SI, Figure S13 and Table S6). Taken together, our analysis demonstrates successful site-specific incorporation of UBPs into RNA-based biosensors by *in vitro* transcription, with little to no mis-incorporation observed.

Having rigorously validated the UBP-containing biosensors, we next determined their fold turn-on and response time. A higher RNA concentration was used in these assays (300 nM) in case the constructs had weak performance. Biosensors with complementary UBPs retain function similar to WT, with fluorescence fold turn-on in the range of 2.9−4.2 (Figure 2B, Table 2). In contrast, biosensors with the Ds-Ds self-pair in the same positions were severely disrupted. The replacement of Pa with Pa′ in the UBP led to higher fold turn-on at U3 and A47 positions but lower fold turn-on at U4 and A46 positions. Highest fold turn-on was observed for the Pa4-Ds46 construct.

Table 2. Fold Turn-On and Kinetic Parameters of UBP Containing P1 Stem Mutants[a]

mutation	ft	$t_{1/2}$ (min)	k_{obs} (min^{-1})	k_{rel}
none (WT)	4.0	2.39 ± 0.20	0.29 ± 0.03	1.0
Pa3-Ds47	3.4	1.59 ± 0.07	0.43 ± 0.02	1.5
Pa′3-Ds47	3.6	1.83 ± 0.22	0.38 ± 0.04	1.3
Ds3-Pa47	2.9	1.64 ± 0.31	0.42 ± 0.04	1.4
Ds3-Pa′47	3.4	1.71 ± 0.22	0.40 ± 0.05	1.4
Pa4−Ds46	4.2	1.69 ± 0.08	0.41 ± 0.03	1.4
Pa′4−Ds46	3.1	1.65 ± 0.21	0.42 ± 0.05	1.4
Ds4−Pa46	4.1	1.99 ± 0.21	0.35 ± 0.04	1.2
Ds4−Pa′46	3.9	1.92 ± 0.11	0.36 ± 0.02	1.2

[a]bp = base pair, ft = fold turn-on $k_{rel} = k_{obs}$(mutants)/ k_{obs} (WT). All measurements were done in duplicate with 300 nM RNA. Standard deviation for fold turn-on was ≤0.3.

Excitingly, all biosensors with complementary UBPs exhibit faster turn-on than WT ($\Delta t_{1/2}$ = 0.4−0.8 min, k_{rel} = 1.2−1.5, SI, Figures S14 and S15 and Table S2). UBP position and orientation (e.g., Pa-Ds or Ds-Pa) had larger effects on kinetics than replacement of Pa with Pa′ in the UBP. Fastest turn-on was observed for Pa3-Ds47 ($\Delta t_{1/2}$ = 0.8 min, k_{rel} = 1.5, Figure 2C, Table 2). Interestingly, this UBP-containing biosensor showed a faster response even though its ligand binding affinity was somewhat reduced (K_D 312 vs 189 μM, SI, Figures S6 and S16).

To directly compare UBP containing biosensors to the natural mutants, select P1 mutants were reanalyzed at higher RNA concentration (SI, Figure S17 and Table S7). Under these conditions, the biosensor mutant C4-G46 remains the fastest natural construct ($\Delta t_{1/2}$ = 0.9 min, k_{rel} = 1.6), which is closely matched by Pa3-Ds47. This result shows that natural base pair mutants can be as effective at disrupting misfolding as the removal of hydrogen-bonding. In addition, we found that systematic mutagenesis, which is simpler to perform with natural base pairs, can identify functional hotspots for UBP incorporation. However, it is possible that UBPs may also be advantageous at different sites. In the future, we would like to investigate whether consecutive UBP incorporation or randomization of UBP in a functional RNA will improve RNA folding.

In summary, here, we show that systematic mutagenesis and/or incorporation of UBPs in the riboswitch aptamer can reveal mutation hotspots and improve response times over the original sequence without compromising ligand binding affinity or fold turn-on. The regulatory function of many riboswitches

https://doi.org/10.1021/acssensors.3c01266
ACS Sens. 2023, 8, 4468−4472

is kinetically controlled and the kinetics of cotranscriptional riboswitch folding and ligand binding affect gene expression.[21,22] In general, RNA ligand association kinetics is slow, happening between millisecond to second time scale, and transcriptional or translational gene regulation happen in seconds to minute time scale.[23−25] Thus, improvement of riboswitch folding and ligand binding by one minute is significant and can potentially impact *in vivo* function. Additionally, many cellular functions like metabolite turnover, transcription, and translation happen in second to minute time scales.[26] Hence biosensors that activate on the minute time scale are useful for sensing such dynamic biological processes. Finally, our studies show that UBP-containing biosensors not only retain function but also exhibit enhanced response rates. Thus, this study supports the idea that incorporation of UBPs into RNA tools may improve their folding and hence their function in the cell. We expect that these strategies can be directly transferred to other riboswitch- and RNA-based devices such as aptazyme and natural and synthetic riboregulators.

■ ASSOCIATED CONTENT

Data Availability Statement

Preprint DOI link: 10.26434/chemrxiv-2023-xlth4.

Supporting Information

The Supporting Information is available free of charge at https://pubs.acs.org/doi/10.1021/acssensors.3c01266.

Experimental materials and methods, supplementary figures and tables (PDF)

■ AUTHOR INFORMATION

Corresponding Authors

Ming C. Hammond − *Department of Chemistry and Henry Eyring Center for Cell & Genome Science, University of Utah, Salt Lake City, Utah 84112, United States;* orcid.org/0000-0003-2666-4764; Email: mingch@chem.utah.edu

Ichiro Hirao − *Institute of Bioengineering and Bioimaging (IBB), A*STAR, 138669, Singapore; Xenolis Pte. Ltd., 118259, Singapore;* orcid.org/0000-0002-1115-8079; Email: ichiro.hirao@xenolis.com

Authors

Sudeshna Manna − *Department of Chemistry and Henry Eyring Center for Cell & Genome Science, University of Utah, Salt Lake City, Utah 84112, United States;* orcid.org/0000-0003-3129-1819

Michiko Kimoto − *Institute of Bioengineering and Bioimaging (IBB), A*STAR, 138669, Singapore; Xenolis Pte. Ltd., 118259, Singapore*

Johnny Truong − *Department of Chemistry and Henry Eyring Center for Cell & Genome Science, University of Utah, Salt Lake City, Utah 84112, United States*

Praneeth Bommisetti − *Department of Chemistry, University of Utah, Salt Lake City, Utah 84112, United States*

Ava Peitz − *Department of Chemistry and Henry Eyring Center for Cell & Genome Science, University of Utah, Salt Lake City, Utah 84112, United States;* orcid.org/0000-0002-4978-3777

Complete contact information is available at: https://pubs.acs.org/10.1021/acssensors.3c01266

Author Contributions

S.M., M.K., J.T., P.B., and A.P. conducted the research, S.M., J.T., and M.K. designed the experiments, S.M., M.K., I.H., and M.C.H. wrote the manuscript, and I.H. and M.C.H. supervised the project. All authors reviewed and edited the manuscript.

Notes

The authors declare the following competing financial interest(s): Authors MK and IH have financial interests in Xenolis Ptd Ltd.

■ ACKNOWLEDGMENTS

We thank Prof. Vahe Bandarian at University of Utah for providing access to the Vanquish UHPLC instrument and Q-exactive mass spectrometers. This work was supported by grants from Office of Naval Research (N000142112188) and the National Institutes of Health (R01 GM124589). The Vanquish UHPLC instrument and Q-exactive mass spectrometer used for RNase T1 digestion analysis was supported by the National Institutes of Health (R35 GM126956).

■ REFERENCES

(1) Kim, C. M.; Smolke, C. D. Biomedical Applications of RNA-Based Devices. *Curr. Opin Biomed Eng.* **2017**, *4*, 106−115.

(2) Thavarajah, W.; Hertz, L. M.; Bushhouse, D. Z.; Archuleta, C. M.; Lucks, J. B. RNA Engineering for Public Health: Innovations in RNA-Based Diagnostics and Therapeutics. *Annu. Rev. Chem. Biomol Eng.* **2021**, *12*, 263−286.

(3) Strack, R. L.; Song, W.; Jaffrey, S. R. Using Spinach-based sensors for fluorescence imaging of intracellular metabolites and proteins in living bacteria. *Nat. Protoc* **2014**, *9* (1), 146−155.

(4) Su, Y.; Hammond, M. C. RNA-based fluorescent biosensors for live cell imaging of small molecules and RNAs. *Curr. Opin Biotechnol* **2020**, *63*, 157−166.

(5) Manna, S.; Truong, J.; Hammond, M. C. Guanidine Biosensors Enable Comparison of Cellular Turn-on Kinetics of Riboswitch-Based Biosensor and Reporter. *ACS Synth. Biol.* **2021**, *10* (3), 566−578.

(6) Strack, R. L.; Disney, M. D.; Jaffrey, S. R. A superfolding Spinach2 reveals the dynamic nature of trinucleotide repeat-containing RNA. *Nat. Methods* **2013**, *10* (12), 1219−1224.

(7) Benner, S. A.; Karalkar, N. B.; Hoshika, S.; Laos, R.; Shaw, R. W.; Matsuura, M.; Fajardo, D.; Moussatche, P. Alternative Watson-Crick Synthetic Genetic Systems. *Cold Spring Harb Perspect Biol.* **2016**, *8*, a023770.

(8) Morales, J. C.; Kool, E. T. Minor Groove Interactions between Polymerase and DNA: More Essential to Replication than Watson-Crick Hydrogen Bonds? *J. Am. Chem. Soc.* **1999**, *121*, 2323−2324.

(9) Henry, A. A.; Romesberg, F. E. Beyond A, C, G and T: augmenting nature's alphabet. *Curr. Opin Chem. Biol.* **2003**, *7* (6), 727−733.

(10) Lee, K. H.; Hamashima, K.; Kimoto, M.; Hirao, I. Genetic alphabet expansion biotechnology by creating unnatural base pairs. *Curr. Opin Biotechnol* **2018**, *51*, 8−15.

(11) Kimoto, M.; Yamashige, R.; Matsunaga, K.; Yokoyama, S.; Hirao, I. Generation of high-affinity DNA aptamers using an expanded genetic alphabet. *Nat. Biotechnol.* **2013**, *31* (5), 453−457.

(12) Zhang, L.; Yang, Z.; Sefah, K.; Bradley, K. M.; Hoshika, S.; Kim, M.-J.; Kim, H.-J.; Zhu, G.; Jiménez, E.; Cansiz, S.; et al. Evolution of Functional Six-Nucleotide DNA. *J. Am. Chem. Soc.* **2015**, *137* (21), 6734−6737.

(13) Glushakova, L. G.; Alto, B. W.; Kim, M.-S.; Hutter, D.; Bradley, A.; Bradley, K. M.; Burkett-Cadena, N. D.; Benner, S. A. Multiplexed kit based on Luminex technology and achievements in synthetic biology discriminates Zika, chikungunya, and dengue viruses in mosquitoes. *BMC Infectious Diseases* **2019**, *19* (1), 418.

(14) Morohashi, N.; Kimoto, M.; Sato, A.; Kawai, R.; Hirao, I. Site-specific incorporation of functional components into RNA by an

unnatural base pair transcription system. *Molecules* **2012**, *17* (3), 2855−2876.
(15) Domnick, C.; Eggert, F.; Wuebben, C.; Bornewasser, L.; Hagelueken, G.; Schiemann, O.; Kath-Schorr, S. EPR Distance Measurements on Long Non-coding RNAs Empowered by Genetic Alphabet Expansion Transcription. *Angew. Chem., Int. Ed. Engl.* **2020**, *59* (20), 7891−7896.
(16) Zhang, Y.; Ptacin, J. L.; Fischer, E. C.; Aerni, H. R.; Caffaro, C. E.; San Jose, K.; Feldman, A. W.; Turner, C. R.; Romesberg, F. E. A semi-synthetic organism that stores and retrieves increased genetic information. *Nature* **2017**, *551* (7682), 644−647.
(17) Hoshika, S.; Leal, N. A.; Kim, M. J.; Kim, M. S.; Karalkar, N. B.; Kim, H. J.; Bates, A. M.; Watkins, N. E., Jr.; SantaLucia, H. A.; Meyer, A. J.; et al. Hachimoji DNA and RNA: A genetic system with eight building blocks. *Science* **2019**, *363* (6429), 884−887.
(18) Hirao, I.; Kimoto, M.; Mitsui, T.; Fujiwara, T.; Kawai, R.; Sato, A.; Harada, Y.; Yokoyama, S. An unnatural hydrophobic base pair system: site-specific incorporation of nucleotide analogs into DNA and RNA. *Nat. Methods* **2006**, *3* (9), 729−735.
(19) Mitsui, T.; Kitamura, A.; Kimoto, M.; To, T.; Sato, A.; Hirao, I.; Yokoyama, S. An Unnatural Hydrophobic Base Pair with Shape Complementarity between Pyrrole-2-carbaldehyde and 9-Methylimidazo[(4,5)-b]pyridine. *J. Am. Chem. Soc.* **2003**, *125* (18), 5298−5307.
(20) Matsunaga, K.; Kimoto, M.; Lim, V. W.; Tan, H. P.; Wong, Y. Q.; Sun, W.; Vasoo, S.; Leo, Y. S.; Hirao, I. High-affinity five/six-letter DNA aptamers with superior specificity enabling the detection of dengue NS1 protein variants beyond the serotype identification. *Nucleic Acids Res.* **2021**, *49* (20), 11407−11424.
(21) Wickiser, J. K.; Winkler, W. C.; Breaker, R. R.; Crothers, D. M. The speed of RNA transcription and metabolite binding kinetics operate an FMN riboswitch. *Mol. Cell* **2005**, *18* (1), 49−60.
(22) Wickiser, J. K.; Cheah, M. T.; Breaker, R. R.; Crothers, D. M. The Kinetics of Ligand Binding by an Adenine-Sensing Riboswitch. *Biochemistry* **2005**, *44* (40), 13404−13414.
(23) Scull, C. E.; Dandpat, S. S.; Romero, R. A.; Walter, N. G. Transcriptional Riboswitches Integrate Timescales for Bacterial Gene Expression Control. *Front Mol. Biosci* **2021**, *7*, 607158.
(24) Al-Hashimi, H. M.; Walter, N. G. RNA dynamics: it is about time. *Curr. Opin Struct Biol.* **2008**, *18* (3), 321−329.
(25) Gleitsman, K. R.; Sengupta, R. N.; Herschlag, D. Slow molecular recognition by RNA. *RNA* **2017**, *23* (12), 1745−1753.
(26) Shamir, M.; Bar-On, Y.; Phillips, R.; Milo, R. SnapShot: Timescales in Cell Biology. *Cell* **2016**, *164*, 1302.

https://doi.org/10.1021/acssensors.3c01266
ACS Sens. 2023, 8, 4468−4472